Non-isothermal kinetics of styrene–butadiene–styrene asphalt combustion*

Wu Ke(吴 珂)[a], Zhu Kai(朱 凯)[a], Han Jun(韩 君)[a,c], Wang Jin-Chang(王金昌)[a], Huang Zhi-Yi(黄志义)[a,†], and Liang Pei(梁 培)[b]

[a] *Faculty of Engineering, Zhejiang University, Hangzhou* 310027, *China*
[b] *College of Optical and Electronic Technology, China Jiliang University, Hangzhou* 310018, *China*
[c] *Jiangsu Bao Li Asphalt Co. LTD, Wuxi* 214422, *China*

(Received 14 August 2012; revised manuscript received 31 October 2012)

The combustion characteristics of styrene–butadiene–styrene (SBS) asphalt are studied by thermogravimetric analysis (TG/DTG) at four different heating rates. According to the saturates/aromatics/resins/asphaltenes (SARA) fractionation method, the combustion process of SBS asphalt can be divided by Gaussian peak fitting into three main stages: oil content release, resin pyrolysis, and asphaltene and char combustion. When the heating rate increases, the mass losses of the oil content and resin pyrolysis increase, and less asphaltenes are formed at a higher temperature. The activation energy values are calculated by the Coats–Redfern method to be in the range 61.6 kJ/mol–142.9 kJ/mol. The Popescu method is used for the kinetic analysis, and the result shows that the three stages of asphalt combustion can be explained by the sphere phase boundary reaction model, the second order chemical reaction model, nucleation, and its subsequent growth model, respectively.

Keywords: SBS asphalt, combustion, non-isothermal kinetic, TG/DTG

PACS: 88.20.jj, 88.05.Np, 88.05.De **DOI:** 10.1088/1674-1056/22/6/068801

1. Introduction

Asphalt is a complex organic compound that is widely used to waterproof roofing systems or to serve as a binder in road construction.[1,2] However, due to its relatively large volatile content, asphalt material can be ignited at a comparatively low temperature (300 °C).[3] Therefore, it has been used in metallurgy as a substitute for coal.[4] In the fire scenario, the temperature is particularly high, and in particular in tunnel fires, the maximum combustion temperature can reach 1000 °C in a few minutes,[5] which can ignite a large area of asphalt. Asphalt combustion releases significant heat and toxic fumes, which seriously endanger any personnel within an affected area. Adequate preventative measures are needed to minimize the ignition risk and subsequent casualties, so it is important to understand how combusting asphalt behaves within the confines of an asphalt fire scenario.

Experimental studies of the kinetics of asphalt combustion have been carried out by several researchers under laboratory settings. Thermogravimetric research is widely used to analyze the mechanism of the solid reaction.[6–9] Gong and Fu[10,11] found that asphalt combustion comprises a pyrolysis stage and a char combustion stage. Benbouzid and Hafsi[4] studied the pyrolysis stage of bitumen at three different heating rates, and the results showed that the reaction order of asphalt pyrolysis approached 1, and the oxidized fraction of bitumen decomposed at low temperatures. Murugan[12,13] proved that the combustion kinetics of asphaltenes in crude oils had an activation energy of 66.73 kJ/mol. Xu and Huang[14,15] studied the combustion of asphalt and modified asphalt. They discovered that the combustion process of asphalt has three main consecutive stages, as the pyrolysis stage can be divided into two stages. The combustion reaction increases in intensity from the first to the third stage, and the reaction order is assumed to be 1 in all three stages. The kinetic models in the majority of the literature for asphalt pyrolysis and combustion are simple reaction order models.[4,11–14]

The chemical composition of asphalt is extremely complex, and according to the SARA fractionation,[16] asphalt components can be grouped into four categories: saturates, aromatics, resins, and asphaltenes.[16] Due to the fact that each component has its own combustion activity, the combustion process of asphalt is multistage, of which each stage is driven by a mechanism that is different from that driving the other stage. This means that the simple kinetic models in use today are not accurate enough to describe the complicated processes that take place in asphalt combustion. Furthermore, asphalt combustion kinetic models are still lacking a deep and systematic study.

In this paper, we investigate the combustion characteristics of styrene–butadiene–styrene (SBS) asphalt in thermogravimetric experiments under different heating rates. The

*Project supported by the National Natural Science Foundation of China (Grant Nos. 61154002 and 51078331), the China Postdoctoral Science Foundation (Grant No. 20090451471), and the Natural Science Foundation of Zhejiang Province, China (Grant No. Z1110222).

†Corresponding author. E-mail: hzy@zju.edu.cn

© 2013 Chinese Physical Society and IOP Publishing Ltd

Popescu method and Gaussian peak fitting are used to analyze the corresponding kinetic parameters. The results reveal the mechanism of asphalt combustion, which is useful for quantitatively evaluating fire safety based on the selection of asphalt materials.

2. Experiment

2.1. Materials

SBS is considered the most appropriate polymer for experiments with asphalt modification[17] since it is a block copolymer that increases the elasticity of asphalt and has been used in highways in China.

The SBS asphalt was produced by the Sinopec Group with a penetration of 67 dmm at 25 °C, a ductility of 40 cm at 5 °C, a softening point of 66-°C kinematic viscosity of 1.7 Pa · s at 135 °C, and a flash point of more than 230 °C.

Table 1 shows the proximate and ultimate analyses of SBS as determined by a LECO-CHNS932 elemental analyzer and a 5E-MACIII infrared fast analyzer.

Table 1. Proximate and ultimate analyses of the samples.

Proximate analysis/wt%, ad		Ultimate analysis/wt%, ad	
Moisture	1.96	Carbon	87.86
Ash	1.64	Hydrogen	5.18
Volatile matter	83.91	Nitrogen	0.66
Fixed carbon	12.49	Sulphur	3.16
		Oxygen	1.5

Note: ad means air dried basis.

2.2. Methods

The experiments were conducted using the thermal analyzer TGA/SDTA 851e (Mettler Toledo, USA and Switzerland). The samples were first heated from room temperature to 1000 °C at four different heating rates of 5, 10, 20, and 30 °C/min, and then heated at a constant temperature of 1000 °C for 15 min. The input gas was composed of 20% oxygen and 80% nitrogen by volume, and the flow rate was kept at 50 ml/min. Approximately 10 mg of the sample was placed in an aluminum oxide crucible with a cross-section area of 4.9×10^{-4} m^2. Before the formal experiments, temperature and balance calibration were performed, and the experiments were done three times under each condition, with the average data used. The results show that the TG curves are superposed perfectly and the error is allowable.

3. Results and discussion

3.1. Thermogravimetric analysis

Four sets of TG experiments were performed to examine the combustion behavior of SBS asphalt, and the mass loss (TG) curve at a heating rate of 20 °C · min^{-1} is shown in Fig. 1.

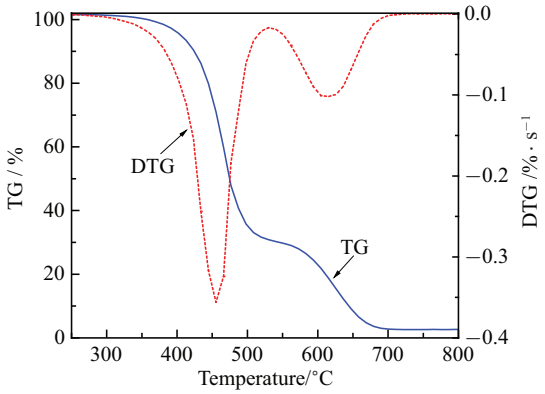


Fig. 1. (color online) The TG and DTG curves of asphalt combustion.

From the differential on the TG curve, we can obtain the DTG curve, which reflects the relationship between the mass loss rate and temperature. In Fig. 1, the DTG curve of asphalt shows significant peaks and shoulders, which can be explained by the linear superposition of the component reactions in asphalt. According to the SARA fractionation, the asphalt components are usually classified into four categories: (I) saturates, (II) aromatics, (III) resins, and (IV) asphaltenes.[16] Each component has its own combustion activity (I & II > III > IV),[18] so each component reaction may correspond to a single mass loss peak.

The Gaussian peak fitting method[19] has been widely adopted in spectral analysis, and can separate the coupled complex peaks effectively by multiple Gaussian peaks. In this paper, Gaussian peak fitting is used to fit the DTG curve of each component. The Gaussian function for fitting can be written as follows:

$$y = y_0 + \sum \frac{A_i}{w_i \sqrt{\pi/2}} \exp\left[-2\frac{(x_i - x_{ci})^2}{w_i^2}\right], \qquad (1)$$

where y_0 is the baseline, and A_i, w_i, and x_i are the peak area, the half-height width, and the peak position of peak i, respectively.

The multi-peak fitting results are shown in Fig. 2 and Table 2.

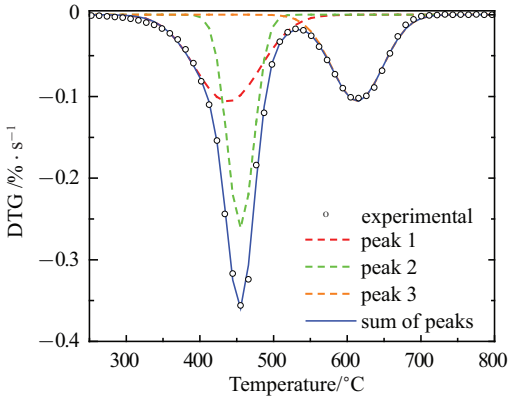


Fig. 2. (color online) The multi-peak fitting of the DTG curve.

Table 2. The different stages of asphalt combustion.

Stages	T_R/°C	T_P/°C	Corresponding reaction
I	350–530	437	release and combustion of oil content
II	405–500	455	pyrolysis and combustion of resins
III	530–680	613	combustion of asphaltenes and char

Note: T_R denotes the reaction region temperature, and T_P the peak temperature.

In Fig. 2, there are two major weight loss peaks on the DTG curve. The mass loss of the first peak (350 °C∼530 °C) is about 70%, which is less than the quantity of volatiles. This mass loss peak is probably related to the release and combustion of a primary volatile. This peak of the primary volatile release can be decomposed into two stages, and the two stages are highly coupled. Stage I is possibly attributed to the release and combustion of oil content (including saturates and aromatics) by the radical polymerization reaction.[20] Due to their smaller molecular weight and lower pyrolysis temperature, the oil content is released at a relatively low temperature. In stage II, the peripheral functional groups and heteroatom bonds are broken, resins are oxidized and dehydrogenated, and then asphaltenes and char are formed. The second peak is ascribed to the release of secondary volatiles and char combustion. Stage III corresponds to the second mass loss peak in the DTG curve, and the temperature range of 530 °C–680 °C. In this stage asphaltenes decompose,[21] the aromatic molecules increase gradually and char comes into being due to the condensation of free radical molecules. The relatively stable char is ultimately burned.

The combustion characteristics at four different asphalt heating rates are shown in Table 3. It indicates that the heating rate has a great influence on asphalt combustion. Figure 3 shows that with the increase in heating rate, the average burning rate grows rapidly. The DTG peak shifts toward higher temperature as the heating rate increases, which is due to the thermal hysteresis produced by the larger heating rate, which would affect the pyrolysis of the inner part of the particles. In addition, when the heating rate increases, the mass losses of stages I and II will increase. This illustrates a lower oil content and resin release at a lower heating rate, which may be attributed to the longer reaction time in the lower heating rate, and more active ingredients cannot diffuse out at the lower temperature but are converted into more stable products such as asphaltenes. In a tunnel fire, the maximum temperature can reach 1000 °C within 5 min. The actual heating rate is much higher than that in the TGA experiment, so more oil content and resin will be released in the tunnel fire. Inhibiting the initial heating rate can suppress the burning of asphalt.

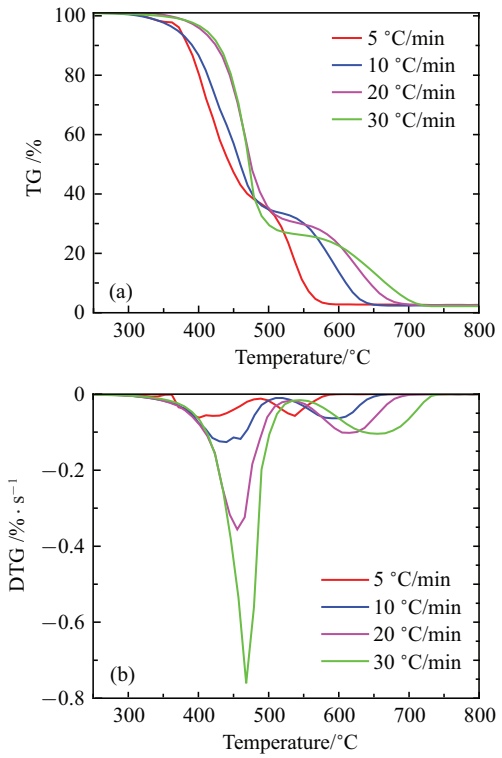


Fig. 3. (color online) TG/DTG curves of asphalt combustion at different heating rates.

Table 3. The combustion characteristics of asphalt at different heating rates.

β/°C · min^{-1}	Burning rate/kg · (m^2 · s)$^{-1}$	Mass loss 1/%	Mass loss 2/%
5	6.18×10^{-6}	63.8	33.2
10	9.69×10^{-6}	66.5	31.2
20	2.39×10^{-5}	69.7	27.2
30	4.90×10^{-5}	73.7	24.2

Note that mass loss 1 refers to the mass losses of stages I and II, and mass loss 2 to the mass loss of stage III.

3.2. Kinetic analysis

Generally, the kinetic equation of the process can be written as follows:

$$d\alpha/dt = k(T)f(\alpha), \tag{2}$$

where α, t, and T are the degree of conversion, time of combustion process, and combustion temperature at moment t, respectively; $f(\alpha)$ is a function, of which the type depends on the reaction mechanism; and $k(T)$ is the temperature dependence of rate constant.

The temperature dependence of the rate constant $k(T)$ is described by the Arrhenius equation, so the kinetic equation may be written as follows:

$$d\alpha/dt = A\exp(-E/RT)f(\alpha), \tag{3}$$

where A is the pre-exponential factor; E is the activation en-

ergy; and R is the universal gas constant.

In these experiments, temperature increases at a constant rate of $\beta = \mathrm{d}T/\mathrm{d}t$. We can change the variable time into temperature:

$$\mathrm{d}\alpha/\mathrm{d}T = (A/\beta)\exp(-E/RT)f(\alpha). \tag{4}$$

By separating the variables and integrating, the following equation is obtained:

$$g(\alpha) = \int_0^\alpha \frac{\mathrm{d}\alpha}{f(\alpha)} = \frac{1}{\beta}\int_0^T A\exp(-E/RT)\mathrm{d}T. \tag{5}$$

The formal expression of the function $g(\alpha)$ depends on the reaction mechanism and its mathematical model, which can be obtained by the Popescu method.[23] This is a multiple scanning rate method from which kinetic models can be derived using experimental data at different heating rates. In addition, the Popescu method not only avoids the difficulties in formula applicability with the kinetic compensation effect,[24] which means that the kinetic function $g(\alpha)$ does not depend on the temperature dependence of rate constant $k(T)$, but it also does not introduce any temperature integration approximation either. The integral term $\int_0^T A\exp(-E/RT)\mathrm{d}T$ is a constant at a certain temperature. By using Eq. (5), a plot of $g(\alpha)$ versus $1/\beta$ would lead to a straight line with an intercept of zero, so the reaction mechanism function can be determined by a best linear regression fit of $g(\alpha)$ versus $1/\beta$.

The kinetic mechanism of asphalt combustion is extremely complicated because of the complex organic components and their parallel reactions. Traditional kinetic models of reaction order are based on the homogeneous reaction, which cannot describe the heterogeneous reaction well.[24] A large number of kinetic models are available for interpreting solid fuel combustion. The mechanism functions of the three stages are considered to be different due to their different reaction types, and the mechanism functions and kinetic parameters are determined by assuming a single separate reaction for each stage. The three stages of asphalt combustion correspond to oil content release, resin pyrolysis, and asphaltene and char combustion.

Vlaev *et al.*[25] listed the kinetic models with good linearity, which can be found in Appendix A. The results of the linear regression fit of $g(\alpha)$ versus $1/\beta$ at the characteristic temperature can be obtained from these kinetic models, where a larger correlation coefficient means a better data fit.

From Fig. 4, the highest correlation coefficient of stage I is obtained by function 11. This indicates that the release and combustion of oil content are accordant with the sphere phase boundary reaction model with power law. For the pyrolysis of resin, the best correlation coefficient of the combustion reaction in stage II is obtained with function 12, indicating that the reaction is a second-order chemical reaction. Finally, function 6 is suitable for the combustion of asphaltenes and char. All these correlation coefficients are larger than 0.985, so the kinetic models are reliable.

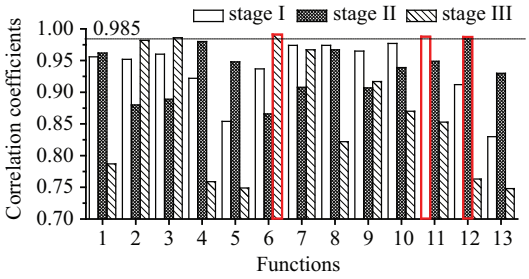


Fig. 4. (color online) The correlation coefficients corresponding to various kinetic mechanisms.

In order to obtain the active energy E and pre-exponential factor A, equation (5) is transformed into the following integral type of equation with the Coats–Redfern method,[26] which has been mostly and successfully used for studying the kinetics of dehydration and the decomposition of different solid substances:

$$\ln\frac{g(\alpha)}{T^2} = \ln\frac{AR}{\beta E} - \frac{E}{RT} + \ln\left(1 - \frac{2RT}{E}\right) \approx \ln\frac{AR}{\beta E} - \frac{E}{RT}. \tag{6}$$

From Eq. (6) it follows that $\ln(AR/\beta E)$ is constant and a plot of $\ln(g(\alpha)/T^2)$ against $1/T$ should be a straight line with slope E/RT, from which the values of E and A can be calculated by using the TG/DTG data.

Table 4 shows that the activation energy varies significantly in each combustion stage, which is due to their different reaction mechanisms. In stage I, the lively volatiles are released by breaking some unstable weak bonds and the active energy is relatively low. The active energy can reflect the difficulty degree of the reaction. The low active energy means that the material is easy to burn. Therefore, when certain kinds of flame retardants are added to inhibit the release of oil content, the ignition and combustion of asphalt will be retarded. Then the resin is dehydrogenated and polymerized. The active energy in stage II is higher than that in stage I. In the third stage, the active energy is 61.6 kJ/mol, which is consistent with the result of Murugan *et al.*[12,13] The active energy of stage III is much lower than that of stage II, so the asphaltenes and the char will burn strongly in this stage.

Table 4. The kinetic factors of asphalt combustion.

Stage I			Stage II			Stage III		
E	A	$G(a)$	E	A	$G(a)$	E	A	$G(a)$
77.3	1.43×10^3	No.11	142.9	1.76×10^8	No.12	61.6	1.10×10^1	No. 6

In order to verify the accuracy of the experiment, a couple of experiments at a heating rate of 40 °C /min are performed with SBS asphalt. As shown in Fig. 5, the results from the kinetic models are consistent with the experimental values. So the kinetic models of SBS asphalt can be considered to be reliable.

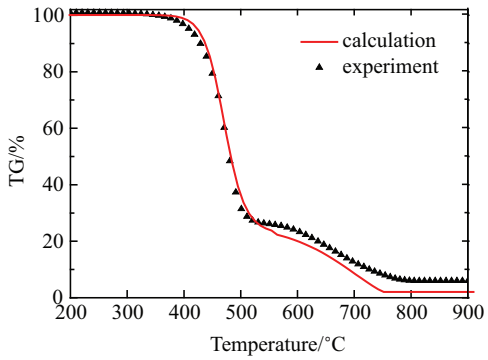


Fig. 5. (color online) Comparison between calculation and experiment.

4. Conclusions

In the present study, we systematically investigated the combustion characteristics of SBS asphalt by thermogravimetric analysis, and the following conclusions were obtained.

(i) Asphalt is a complex compound with several different fractions, and each fraction has its own combustion activity. In this work it is found that there are three main stages in the combustion process of SBS asphalt: oil content release, resin pyrolysis, and asphaltene and char combustion. Stage I is a solid-state reaction, which is well described by the sphere phase boundary reaction model: $\mathrm{d}\alpha/\mathrm{d}T = (4.29 \times 10^3/\beta)\exp(-9.30 \times 10^3/T)(1-\alpha)^{2/3}$, $623 \leq T \leq 803$. Stage II complies with the second-order chemical reaction model: $\mathrm{d}\alpha/\mathrm{d}T = (1.76 \times 10^8/\beta)\exp(-17.2 \times 10^3/T)(1-\alpha)^2$, $678 \leq T \leq 773$. Stage III is a gas–solid reaction, which accords with the nucleation, and its subsequent growth model is $\mathrm{d}\alpha/\mathrm{d}T = (33/\beta)\exp(-7.41 \times 10^3/T)(1-\alpha)[-\ln(1-\alpha)]^{2/3}$, $803 \leq T \leq 953$.

(ii) The activation energies of the three stages are proved to be 77.3, 142.9, and 61.6 kJ/mol, respectively. To significantly improve the flame retardation of asphalt, the oil content release should be inhibited due to its low corresponding active energy and low reaction temperature (350 °C–530 °C).

(iii) The oil content and resin can be converted into more stable content as asphaltenes and char at relatively low temperature, and a low heating rate can extend the reaction time at low temperatures. Therefore, inhibiting the initial heating rate can promote the formation of stable contents and suppress the burning of asphalt.

Acknowledgment

The authors would like to thank Dr. Hao Wu at the Technical University of Denmark for his suggestions on revising this article.

Appendix A

Table A1. Algebraic expressions of the functions $g(\alpha)$ and $f(\alpha)$, and their corresponding mechanisms.[25]

No.	Rate-determining mechanism	$g(\alpha)$	$f(\alpha)$
1	One-dimensional diffusion (Parabola law)	α^2	$1/2\alpha$
2	Two-dimensional diffusion (Valensi equation)	$\alpha+(1-\alpha)\ln(1-\alpha)$	$[-\ln(1-\alpha)]^{-1}$
3	Three-dimensional diffusion (Jander equation)	$[1-(1-\alpha)^{1/3}]^{1/2}$	$6(1-\alpha)^{2/3}[1-(1-\alpha)^{1/3}]^{1/2}$
4	Three-dimensional diffusion (Jander equation)	$[1-(1-\alpha)^{1/3}]^2$	$3/2(1-\alpha)^{2/3}[1-(1-\alpha)^{1/3}]^{-1}$
5	Three-dimensional diffusion (Z–L–T equation)	$[(1-\alpha)^{-1/3}-1]^2$	$3/2(1-\alpha)^{4/3}[(1-\alpha)^{-1/3}-1]^{-1}$
6	Nucleation and its subsequent growth (Avrami–Erofeev equation)	$[-\ln(1-\alpha)]^{1/3}$	$3(1-\alpha)[-\ln(1-\alpha)]^{2/3}$
7	Nucleation and its subsequent growth (Avrami–Erofeev equation)	$[-\ln(1-\alpha)]^{1/2}$	$2(1-\alpha)[-\ln(1-\alpha)]^{1/2}$
8	Nucleation and its subsequent growth (Avrami–Erofeev equation)	$-ln(1-\alpha)$	$1-\alpha$
9	Contracting disk (power law)	α	$(1-\alpha)^0$
10	Contracting cylinder (power law)	$1-(1-\alpha)^{1/2}$	$2(1-\alpha)^{1/2}$
11	Contracting sphere (power law)	$1-(1-\alpha)^{1/3}$	$3(1-\alpha)^{2/3}$
12	Second-order chemical reaction	$(1-\alpha)^{-1}-1$	$(1-\alpha)^2$
13	Third-order chemical reaction	$(1-\alpha)^{-2}-1$	$(1-\alpha)^3$

References

[1] Barral M, Garmendia P, Muñoz M E, Palmillas Z, Romera R and Santamaria A, Villanueva S 2012 *Construction and Building Materials* **30** 650

[2] Tekalur S A, Shukla A, Sadd M and Lee K W 2009 *Construction and Building Materials* **23** 1795

[3] Yu J Y, Cong P L and Wu S P 2009 *Construction and Building Materials* **23** 2277

[4] Benbouzid M and Hafsi S 2008 *Fuel* **87** 1585

[5] Lönermark A and Ingason H 2005 *Fire Safety Journal* **40** 506

[6] Zhang Y M, Han R Q, Wu X S and Wang Z H 2011 *Chin. Phys. Lett.* **28** 128202

[7] Zong F J, Ma H L, Liang W, Du W, Zhang X J, Xiao H D, Ma J, Ji F, Xue C S and Zhuang H Z 2005 *Chin. Phys. Lett.* **22** 907

[8] Huang P, Cui C E and Wang S 2009 *Chin. Phys. B* **18** 4524
[9] Wang L Y, Liu B, Song Z T, Liu W L, Feng S L, Huang D and Babu S V 2011 *Chin. Phys. B* **20** 038102
[10] Gong J S and Fu W B 2003 *Journal of Fuel Chemistry and Technology* **31** 181 (in Chinese)
[11] Gong J S, Fu W B and Zhong B J 2003 *Fuel* **82** 49
[12] Murugan P, Mahinpey N, Mani T and Freitag N 2009 *Fuel* **88** 708
[13] Murugan P, Thilakavathi M, Nader M and Asghari K 2011 *Fuel* **92** 1056
[14] Xu T and Huang X M 2010 *Fuel* **89** 2185
[15] Xu T and Huang X M 2010 *Journal of Analytical and Applied Pyrolysis* **87** 217
[16] Aske N, Kallevik H and Sjöblom J 2001 *Energy & Fuels* **15** 1304
[17] Yildirim Y 2007 *Construction and Building Materials* **21** 66
[18] Guo A J, Zhang X J and Wang Z X 2008 *Fuel Processing Technology* **89** 643
[19] Mukoyama T 1975 *Nucl. Instrum. Method* **125** 289
[20] Kok M V and Karacan C O 2000 *SPE Reservoir Evaluation & Engineering* **3** 380
[21] Gonçlves M L A, Teixeira M A G, Pereira R C L, Mercury R L P and Matos J R 2001 *Journal of Thermal Analysis and Calorimetry* **64** 697
[22] Xu Q 1999 *Acta Phys. Sin.* **48** 16 (in Chinese)
[23] Popescu C 1996 *Thermochimica Acta* **285** 309
[24] Hu R Z and Shi Q Z *Thermal Analysis Kinetics* 1 (Beijing: Science Press) pp. 144–173 (in Chinese)
[25] Vlaev L, Nedelchev N, Gyurova K and Zagorcheva M 2008 *Journal of Analytical and Applied Pyrolysis* **81** 253
[26] Coats A W and Redfern J P 1964 *Nature* **201** 68